estimated by measuring its position relative to the maximum observable half-width of the spectrum's base. This assumes that the spectrum extends to the limb of the planet. If this is not the case, the longitude of the detail will be overestimated, and thus we will overestimate the rotation rate.

Using a composite spectrum constructed by averaging the spectra of 7, 8, 9 and 10 November, we estimate that the longitude of the topographic detail is 23° ± 3°. The given set of spectra was chosen because it fell in the middle of the period of the best position estimates of the detail. The latitude of the detail cannot be estimated from current data, but we have assumed that it is 23° as well. Fortunately, the derived rotation rate varies as the square root of the secant of the latitude and longitude; hence the rate is insensitive to the detail's position if the detail is within 45° of the center of the disk.

The estimated rate at which the detail was moving across the spectrum for the week prior to conjunction is

$$0.28 \begin{array}{l} +0.30 \\ -0.10 \end{array} \text{ cy/day.}$$

This rate corresponds to an apparent angular velocity of

$$\left(2.0 \begin{array}{l} +0.87 \\ -0.41 \end{array} \right) \times 10^{-7} \text{ radian/sec.}$$

Synchronous rotation would be approximately 4.4×10^{-7} radian/sec. The apparent angular velocity of Venus is the projection onto a plane perpendicular to the line of sight of the sum of two components: (i) a component due to the rotation of Venus on its own axis and (ii) a component due to an apparent rotation caused by Venus passing the earth in space. If it is assumed that the axis of Venus is perpendicular to its orbit, then the angular velocity found corresponds to a sidereal rotation period of over 1000 days forward or 230 (+40 or −50) days retrograde. The 1000 days forward can be rejected because it leads to spectral bandwidths of about 20 cy/sec for periods of several weeks before and after conjunction, and such a narrow bandwidth was not observed.

The effects of different orientations of the axis are under study; however, a tip of nearly 70° toward the earth would be required to give the same apparent angular velocity if Venus were rotating synchronously (227 days forward). The axis would have to be tipped even more for faster rotation rates.

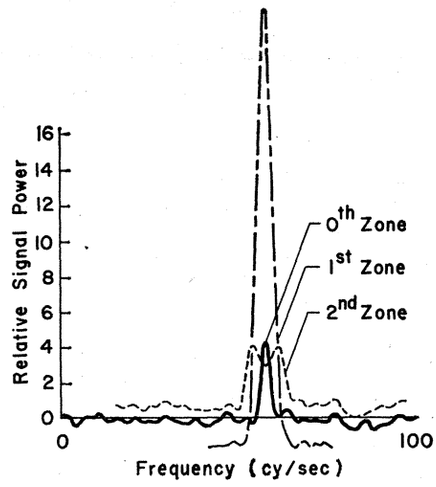

Fig. 3. Spectra of the range-gated zones.

Combining a range-gate with spectral analysis enables one to measure directly the component of Venus rotation which is perpendicular to the line of sight. This is so because the range-gate (a device which accepts echoes from a specified distance, but rejects closer and farther echoes) selects a known portion of the surface of Venus; and the spectrometer, utilizing the Doppler effect, measures the line-of-sight velocity of that portion.

The range-gate operates by modulating the transmitter with a wide-band waveform and modulating the received signal by the waveform's inverse (delayed by the time of flight). Echoes from the proper distance thus pass through the system unaltered, but they remain wide-band from other distances and may be removed with filters.

The true period of rotation of Venus is inferred from several measurements of the perpendicular component, spaced over an interval of several weeks. A rotation period of 250 days, retrograde, fits the data very well, under the assumption that the axis of rotation is perpendicular to the orbit.

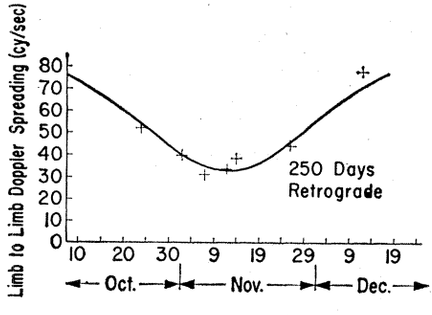

Fig. 4. The limb-to-limb Doppler spreading derived from the spectra of the range-gated zones. The curve shows the expected change assuming a period of 250 days retrograde.

Figure 3 is a sample of the raw data. The reflection from the cap, or zone one, contains most of the power. The bandwidth is remarkably narrow. The echo from the first annular ring, zone two, shows the characteristic double hump and increased Doppler broadening. We used the width of this curve to determine the angular velocity component. Zone zero is the area just ahead of the planet. Normally there would be no power from this zone. However, the range-gate was misaligned slightly to allow the position of the range-gate to be calibrated from the amount of power in zone zero. The distance between zones was 111 miles. These spectrograms required 3 hours of integration time.

Figure 4 shows how well the theoretical curve, calculated from the earth and Venus ephemerides, fits the data. The ordinate is angular velocity, measured in cycles per second of Doppler spreading (limb to limb).

R. M. Goldstein
R. L. Carpenter
Jet Propulsion Laboratory, California Institute of Technology, Pasadena

15 January 1963

Nuclear Explosions: Some Geologic Effects of the Gnome Shot

An unusual byproduct of the underground nuclear explosion at Project Gnome was the development of intrusive breccia veins composed of black salt containing minerals created by the blast. They are associated with complex thrust faulting in the rocks adjacent to the shot-formed cavity. These veins closely resemble ore-bearing breccia pipes, dikes, and veins in some of the western mining camps.

Project Gnome was a multiple-purpose experiment conducted by the U.S. Atomic Energy Commission as part of the Plowshare Program to develop peaceful uses for nuclear explosives. The experiment consisted of the explosion of a nuclear device of about 3-kiloton yield (equivalent to 3,000 tons of TNT) on 10 December 1961. The device was detonated at a depth of about 1200 feet below the surface in a thick salt deposit about 25 miles southeast of Carlsbad, New Mexico.

The device was placed in a 7- by 7-

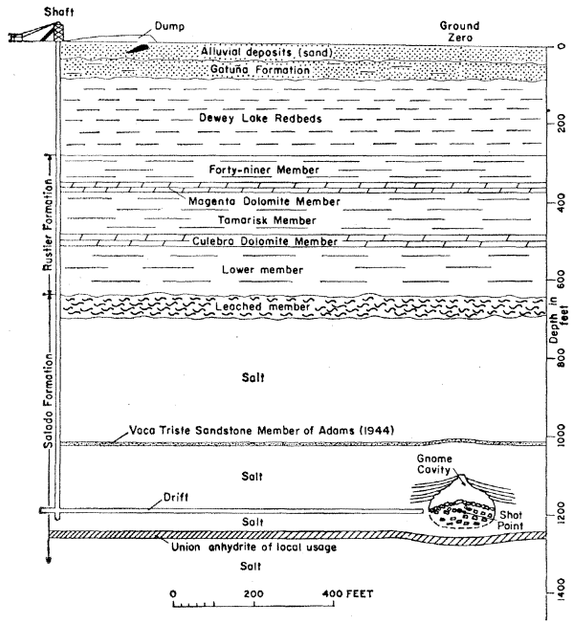

Fig. 1. Geologic cross section between shaft and cavity, Project Gnome.

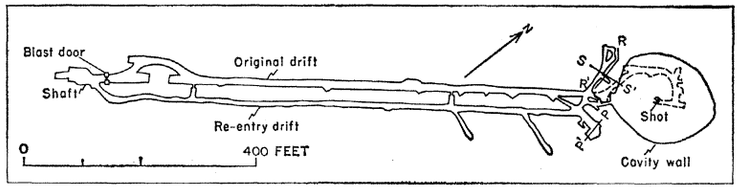

Fig. 2. Plan map of underground workings and cavity showing locations of geologic cross sections (Figs. 3–5).

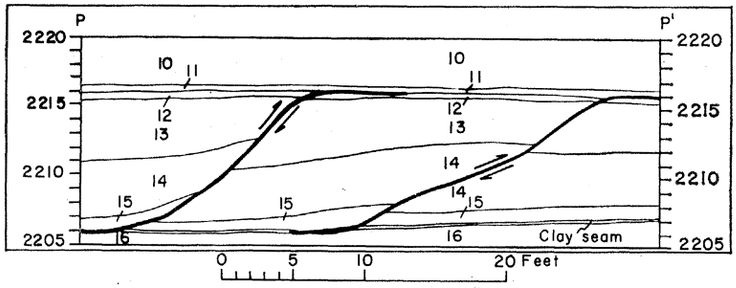

Fig. 3. Geologic cross section *P–P'* of drilling alcove, showing thrust faults. The numbered beds are described in the text. The shot point is to the left.

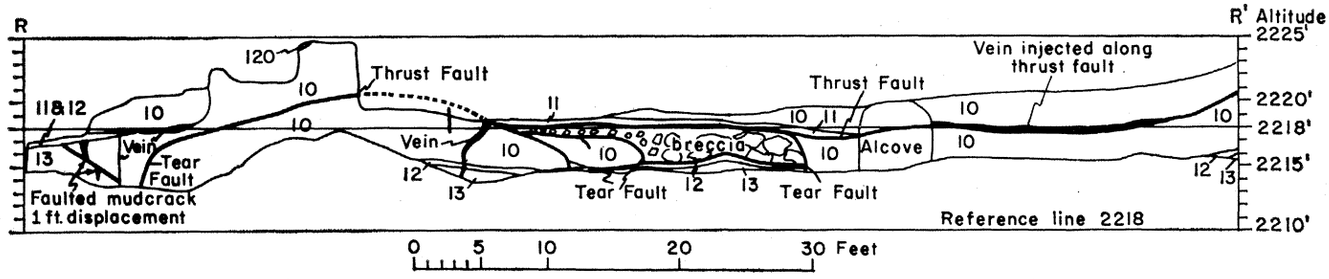

Fig. 4. Geologic cross section *R–R'* along right rib of button-hook reentry drift. Numbered beds are described in the text. Looking toward shot point.

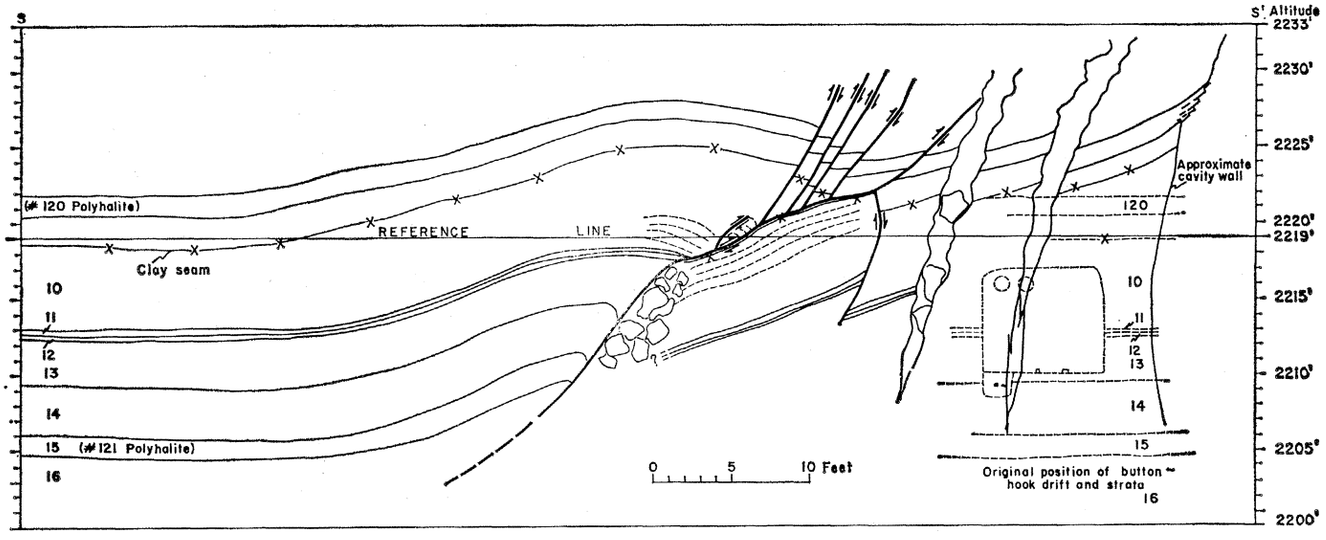

Fig. 5. Geologic cross section *S–S'* through button-hook reentry drift. The numbered beds are described in the text. The shot point is to the right.

by 8-foot chamber at the end of a button-hook-shaped drift designed to be self-sealing. An open cavity about 70 feet high and more than 150 feet across resulted from the blast and from post-shot collapse (Figs. 1 and 2). The ground surface was permanently domed upward for about 400 feet radially around ground zero with a maximum displacement of 1.9 feet. The approximate volume of the domed strata is about 25,000 cubic yards. Post-shot drilling indicates that strata 200 feet above the shot point were permanently displaced 5 feet upward (*1*) and strata 55 feet below the shot point were displaced downward more than 10 feet (*2*). The drilling indicates that no large pool of melted salt was created, although melted salt is distributed between rubble fragments in the bottom of the cavity.

Post-shot geologic investigations by the U.S. Geological Survey revealed that explosion-induced effects included many thrust faults of small displacement. Pre-shot mapping of the original underground workings afforded a background in detailed stratigraphy that proved invaluable in post-shot mapping of structural features. This knowledge of the stratigraphic details enabled me to establish on sight the beds from which each block and fragment originated and to determine accurately the amount of movement along many of the faults.

Rock cover over the device chamber consisted of 500 feet of salt of the Salado Formation of Late Permian age which is overlain by 700 feet of younger sedimentary rocks of the Rustler Formation and Dewey Lake Redbeds of Late Permian age as well as the Gatuña Formation of Pleistocene(?) age, and the alluvial deposits of Quaternary age.

The Salado Formation consists of nearly flat-lying, unfaulted, bedded halite and a few thin beds of clayey halite, anhydrite, polyhalite, and clay. The halite beds range from clear through white to reddish orange. The shade of orange is dependent upon the amount of disseminated polyhalite. The clayey halite beds range from reddish brown to greenish gray. The reddish-brown polyhalite beds, locally used as marker beds, average about 1 foot thick and commonly have a thin bed of greenish-gray clay at the base. Six mappable beds of halite and two beds of polyhalite are exposed in the underground workings, and were arbitrarily numbered in descending order from 9 through 16. Unit 13 contains numerous vertical mudcracks, many of which could be correlated across faults. Unit 9, which was exposed only in the shaft and in post-shot workings, is a polyhalite bed that locally is called No. 120 marker bed. Unit 15, also polyhalite, is marker bed No. 121 of local usage.

The explosion had surprisingly limited effect on the strata lying at the same altitude as the shot point. The principal horizontal effect was outward displacement of rock salt along faults and bedding planes. The displacement is largely confined to a radial distance of about 140 feet from the shot point, although curving vertical faults with slight horizontal movement, concave towards the original drift, are found as far away as 230 feet from the shot point.

Except for radial fractures seen in the explosion-produced cavity, blast-produced faults in the confined salt appear to be restricted to a 10-foot-thick section of salt bounded above and below by clayey layers. These are thrust faults that dip both toward and away from the cavity and die out in the clay layers (Fig. 3). The thrust faults die out laterally by curving downward into vertical tear faults that die out in the salt beds (Fig. 4). The clay layers display slickensides that generally are radial to the shot point. Few of the faults observed had more than a few feet of displacement. Total lateral displacement 100 feet from the shot point as determined by a resurvey of grout-filled instrument holes appears to be about 16 feet radially away from the shot point; at least part of this displacement may be due to plastic deformation, although such deformation is not obvious. Lateral displacement at the shaft 1000 feet from the shot point is 3.5 cm.

The conclusions presented here are, of course, limited to what could be seen within post-shot mine workings. The blast effects undoubtedly extend above and below the present underground workings.

On the west side of the cavity, complex thrust faulting (Fig. 4) accompanied by intrusive breccia is found as far as 110 feet from the shot point. This intense faulting and brecciation (Fig. 5) is believed to be due to the presence of the open button-hook drift, because neither is seen on the south side of the cavity where no openings existed at the time of the shot.

Fig. 6. Intrusive breccia in button-hook drift.

The breccia consists of fragments largely composed of salt from unit 10 that range from a few millimeters to several tens of feet across. These salt fragments occur in a matrix of black salt (Fig. 6). The intrusive breccia contains twisted fragments of mine rail, steel ventilation pipe, wire, aluminum conduit, cable covering, and a few slightly scorched wood fragments. These fragments now are about 35 feet from their original position. Salt in the blocks was granulated but not melted by the shock. Bedding planes are distinct, but where the beds contained halite crystals 10 to 20 mm in size before the blast, the blocks presently are composed of granulated halite crystals 1 mm or less in size. Such intensely granulated zones are not seen elsewhere, even in the cavity walls.

Associated with the blocks of granulated salt are black veins of intrusive breccia containing man-made minerals. These veins are not radioactive. The veins, seldom more than a few inches wide and generally radial to the shot point, display sharp contacts with the host rock and may or may not have been intruded along faults (Fig. 7). The

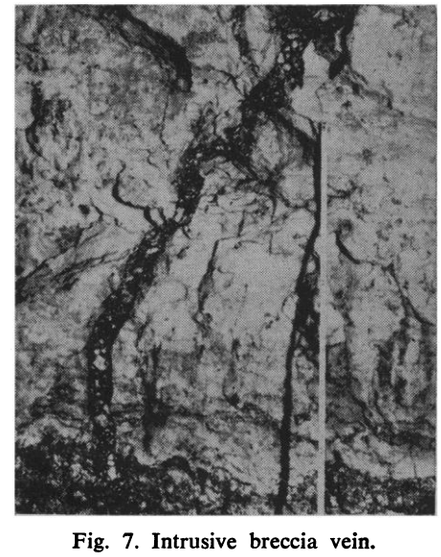

Fig. 7. Intrusive breccia vein.

veins consist of melted and recrystallized salt and contain minute, opaque black minerals disseminated between the salt crystals and sharp-bordered fragments of clear, unmelted, plastically deformed salt. Some of the unmelted salt fragments have a very thin selvage suggesting partial melting, and many of the fragments show warping and bending of bedding and cleavage suggesting plastic deformation. In one thin section a tiny vein displays flow textures with warped and swirled fragments reminiscent of that commonly seen in welded tuffs. Tiny fragments of copper and steel wire are not uncommon constituents.

About 15 percent by weight of samples of the vein material is insoluble in water and consists of opaque black minerals, a few doubly terminated quartz crystals, and a micaceous mineral—probably muscovite. Slight effervescence in acid indicates that some carbonate is present.

X-ray diffractometer patterns of the residue, studied by Theodore Botinelly of the Geological Survey, indicate the presence of the lead minerals laurionite (*3*) (lead hydroxide-chloride) and galena (lead sulfide). Lead in these minerals was derived from lead block used in the device performance measurements (*4*). The extent of distribution of the lead minerals is not known. The samples analyzed came from 100 to 110 feet from the shot point.

About 6 percent of the insoluble residue is carbon which was derived, at least in part, from organic material present in the device chamber at shot time. The quartz and mica were derived from impurities present in the pre-shot salt. No significant increase in iron was found over that contained in pre-shot samples, although a large quantity of iron was present near the device and was vaporized by the blast. The lead combined with chlorine from the sodium chloride and with water to form laurionite and with sulfur derived from the sulfate mineral polyhalite to form the galena. Copper content has increased from about 0.003 percent to 0.7 percent, perhaps owing to the contained wire fragments.

The presence of the OH radical in the laurionite suggests that the mineral was formed at a temperature of less than 142°C, above which point laurionite breaks down into lead chlorides and lead oxides. The components lead and chlorine probably were injected in a vapor state through openings that were closed immediately thereafter. They were deposited in fractures in the cooler portions of the salt. Surviving plastic and rubber cable covering and scorched wood fragments as well as unmelted bits of fine copper wire indicated that the temperature here could not have been very high. The melted salt may have been formed locally by extremely high pressures between the button-hook drift and the shot point or possibly by direct contact with heat released from the device.

Thin sections of the veins show that the melt has narrow chill borders where it is in contact with many of the larger fragments and wall rock. The chill borders are relatively free of lead minerals, whereas the interior of the veins contains the minerals as dust lying between the tiny crystals of melted salt (*5*).

LEONARD M. GARD
U.S. Geological Survey,
Denver 25, Colorado

References and Notes

1. Written communication from the Lawrence Radiation Laboratory, 19 January 1962.
2. Oral communication from T. S. Sterrett, U.S. Geological Survey.
3. Laurionite was first found at Laurium, Greece, where it is formed by the action of seawater on slags from lead mines operated during the time of Pericles (4th century B.C.).
4. A semiquantitative spectrographic analysis of the residue shows a small amount of silver. The presence of silver suggests that the lead used in shielding the device came from a smelter in the western United States.
5. Publication authorized by the director, U.S. Geological Survey. Work done on behalf of the U.S. Atomic Energy Commission.

15 January 1963

Plasma Protein Synthesis in the Liver: Method for Measurement of Albumin Formation in vivo

Abstract. *l-Arginine labeled with carbon-14 at the guanido group was injected into rabbits, and the ratio of the rates of entry of radioactivity into the protein and urea was determined. This ratio, multiplied by the rate of arginine utilization in urea synthesis and by the ratio of protein to protein arginine weights, gives the rate of protein synthesis. The method applies to albumin and should apply to any plasma protein synthesized in those liver cells which also synthesize urea.*

At present, though rates of synthesis of plasma proteins in the steady state in animals can be measured indirectly by determining catabolic rates with proteins labeled with I^{131} they cannot be measured over short periods of time, nor when synthetic and catabolic rates are unequal. The method reported here avoids these disadvantages. Its kinetic basis is defined in Fig. 1; All symbols are defined in the legend. Albumin is used as an example of a protein to which the method applies.

Figure 1 shows three interlinked systems: *system 1*, consisting of arginine in the liver, receiving arginine from the plasma; *system 2*, comprising the albumin in the plasma, in the interstitial fluids and at catabolic sites; and *system 3*, consisting of the urea in the body fluids and that passed into the urine. Present evidence is that essentially all the urea of *system 3* is formed from the guanidine portion of the arginine of *system 1* (*1*), and that all plasma albumin is synthesized in the liver (*2*) so that the albumin of *system 2* receives its arginine from *system 1*. All symbols are explained in the legend of Fig. 1. The albumin of *system 2* consists of that in the plasma, A_∞, that in the interstitial fluids, A_u, and that passing to the catabolic sites. Albumin passes from the plasma to the interstitial fluids at a rate of k_1A_∞ per day and to the catabolic sites at a rate of k_3A_∞ per day. These rates have been measured with I^{131}-albumin in healthy men (*3*, *4*) and rabbits (*5*).

Figure 1 shows that the amount of liver arginine, $A(t_0,t_1)$, entering the plasma albumin of *system 2* in the interval t_0,t_1 is given by

$$A(t_0,t_1) = k_a \int_{t_0}^{t_1} L(t)\,dt \qquad (1)$$

where the symbols are defined in the legend of Fig. 1. If n is the ratio of the number of milligrams of albumin to the number of milligrams of arginine in albumin, then $nA(t_0,t_1)$ is the quantity of albumin synthesized between t_0 and t_1 which we wish to measure.

Figure 1 also shows that the amount of liver arginine required for the synthesis of the urea, $U(t_0,t_1)$, of *system 3* formed between t_0 and t_1 is

$$2.9\,U(t_0,t_1) = k_u \int_{t_0}^{t_1} L(t)\,dt \qquad (2)$$

where 2.9 is the ratio of the molecular weight of arginine to the molecular weight of urea. The quantity $U(t_0,t_1)$ is easily measured, provided bacterial destruction of urea is blocked, as shown in the legend of Fig. 1.

When arginine labeled in the guanidocarbon (arginine-G-C^{14}) is injected in-